SARS-CoV-2 infection paralyzes cytotoxic and metabolic functions of immune cells

Yogesh Singh[1,2,6*,#], Christoph Trautwein[3*], Rolf Fendel[4*], Naomi Krickeberg[4], Jana Held[4], Andrea Kreidenweiss[4], Georgy Berezhnoy[3], Rosi Bissinger[5], Stephan Ossowski[1,2], Madhuri S. Salker[6], Nicolas Casadei[1,2], Olaf Riess[1,2#] and the Deutsche COVID-19 OMICS Initiative (DeCOI)

[1]Institute of Medical Genetics and Applied Genomics, University of Tübingen, Calwerstrasse 7, 72076, Tübingen, Germany

[2]NGS Competence Center Tübingen (NCCT), University of Tübingen, Calwerstrasse 7, 72076 Tübingen, Germany

[3]Werner Siemens Imaging Center, University of Tübingen, Röntgenweg 13, 72076, Tübingen, Germany

[4]Institute of Tropical Medicine, University Hospital of Tübingen, Tübingen, Wilhelmstrasse 27, 72076, Tübingen, Germany

[5]Department of Internal Medicine, Division of Endocrinology, Diabetology and Nephrology, University Hospital of Tübingen, Germany

[6]Research Institute of Women's Health, University of Tübingen, Calwerstrasse 7/6, 72076, Tübingen, Germany

*Equal contributions

Correspondence
Dr Yogesh Singh or Prof Olaf Riess
Institute of Medical Genetics and Applied Genomics, Tübingen University
Calwerstraße 7, 72076, Tübingen, Germany
Phone: 0049 7071 29 72257/78264 Fax: 0049 7071 29 25355
Email: yogesh.singh@med.uni-tuebingen.de or olaf.riess@med.uni.tuebingen.de

Key words: COVID-19, CD8+ T cells, Granzyme B, Perforin, Metabolites

Short title: Defective immune-metabolic functions in COVID-19 patient

Abstract:

The SARS-CoV-2 virus is the causative agent of the global COVID-19 infectious disease outbreak, which can lead to acute respiratory distress syndrome (ARDS). However, it is still unclear how the virus interferes with immune cell and metabolic functions in the human body. In this study, we investigated the immune response in 10 acute or convalescent COVID19 patients. We characterized the peripheral blood mononuclear cells (PBMCs) using flow cytometry and found that $CD8_+$ T cells were significantly subsided in moderate COVID-19 and convalescent patients. Furthermore, characterization of $CD8_+$ T cells suggested that patients with a mild and moderate course of the COVID-19 disease and convalescent patients have significantly diminished expression of both perforin and granzyme B in $CD8_+$ T cells. Using $_1$H-NMR spectroscopy, we characterized the metabolic status of their autologous PBMCs. We found that fructose, lactate and taurine levels were elevated in infected (mild and moderate) patients compared with control and convalescent patients. Glucose, glutamate, formate and acetate levels were attenuated in COVID-19 (mild and moderate) patients. Our findings reveal patients who suffer from an over activation of the immune system, a change of composition in infusion/intravenous fluids during infection with the aim to lower blood levels of glucose, glutamate, acetate and formate could avoid a life-threatening cytokine storm. In summary, our report suggests that SARS-CoV-2 infection leads to disrupted $CD8_+$ T cytotoxic functions and changes the overall metabolic functions of immune cells.

Introduction:

The first cases of severe acute respiratory coronavirus-2 (SARS-CoV-2) infection appeared in December 2019, in Wuhan, China[1]. This zoonotic virus has infected by now more than 26.1 million people (03.09.2020) and killed more than 0.86 million[2,3] worldwide. The containment of the pandemic is challenging and is still continuing with roughly 200,000 or more new infections being reported daily since July 2020[2,3]. There is an urgent need for a better understanding of the immunopathology, as SARS-CoV-2 has become the leading cause of morbidity and mortality in many countries.

Coronaviruses (CoV) are a large family of viruses that can cause illnesses such as the common cold and seasonal influenza[4]. Pathologically, SARS-CoV-2 infects angiotensin-converting enzyme 2 (ACE2)-expressing nasal epithelial cells in the upper respiratory tract and type II alveolar epithelial cells in patients exhibiting pneumonitis[1,5]. The most severe disease courses led to death frequently but not exclusively in older patients with and without risk conditions. The primary symptoms of SARS-CoV-2 infections are fatigue, fever, sore throat, dry cough, loss of smell and taste within 5-21 days of incubation of the virus[6-9]. COVID-19 symptoms are heterogeneous and range from asymptomatic to mild, moderate, and severe pathological symptoms, presenting with or without pneumonia[10,11], however, most infected people develop mild to moderate illness and recover without hospitalization[12,13]. Primarily the older COVID-19 patients can develop acute severe respiratory distress syndrome (ARDS) due to a cytokine storm which is a life-threatening situation, requiring ventilation and intensive care support[14-18]. High serum levels of IL-6, IL-8, IL-10, TNF-α cytokines and an immune hyper-responsiveness referred to as a 'cytokine storm' is connected with poor clinical outcome[19,20].

Several break-through discoveries have extended our understanding how the virus takes advantage of the host and modulates immunity[12,17,21-25]. Recovered COVID-19 patients have an increased number of antibody-secreting cells, activated $CD4_+$ and $CD8_+$ T cells, and immunoglobulin M (IgM) and SARS-CoV-2 reactive IgG antibodies were detected in blood before full symptomatic recovery[26-28]. Most severely affected COVID-19 patients had a lower T cell but elevated B cell counts[13,19,29,30]. Interestingly, patients with mild symptoms were shown to have increased T and B cells compared with severely affected patients[26,29-31]. There could be several reasons for different disease outcomes including over-activated innate or hyper-activated adaptive immune responses leading to cytokine storms and resulting in severe injury to the lungs[10,13,25,32]. Despite of several ongoing efforts, the immunological mechanisms of the host-pathogen interaction are not well understood[33].

There is an intricate balance between the metabolic state of immune cells and generation of immune response[17,34-37]. $CD8_+$ T cells require energy to proliferate and accomplish their effective functions[38]. Most propagating cells such as lymphocytes utilize the most abundant energy substrates including, glucose, lipids, and amino acids[39]. In response to SARS-CoV-2 and other virus infections, $CD8_+$ T cells play a pivotal role in profound growth and proliferation to generate their effective functional cells which can produce copious amounts of effector molecules such as cytokines and cytotoxic granules[30,38-40]. An activated immune system is coupled with a change in metabolic reprogramming to produce enough energy needed during (viral) infection[38,39]. Proliferating T cells ferment glucose to lactate even in the presence of oxygen to meet high energy demands[34,37-39]. Furthermore, glucose and glutamine are involved in the hexosamine biosynthetic pathway, which regulates the production of uridine

144 diphosphate N-acetyl glucosamine necessary for T cell clonal expansion and function[41]. The
145 synthesis of lactate intracellularly is crucial for T cells to have an increased glycolytic flux[38].
146
147 Peripheral blood mononuclear cells (PBMCs) can be analyzed to measure the health status
148 of an individual and can serve as a health biomarkers[42]. Therefore, the metabolic status of
149 lymphocytes could help to predict disease severity or to select the optimal therapeutic
150 intervention to boost the immune function during infection. Generally, most of the metabolism-
151 related functions in PBMCs during SARS-CoV-2 infections were inferred based on
152 transcriptomics analysis[34,43] and no functional data (biochemical level) have been presented.
153 Thereof, understanding the kinetics of adaptive immune response as well as the metabolic
154 functions during SARS-CoV-2 infections will help to elucidate the host immune response to
155 SARS-CoV-2 infection. In this study, using flowcytometry and proton nuclear magnetic
156 resonance (^{1}H-NMR) spectroscopy, we characterized the PBMCs from SARS-CoV-2 infected
157 and convalescent patients for the their immunophenotypic and metabolic functions.
158
159 **Results:**
160
161 *Characteristics of study participants*
162
163 PBMCs were isolated and cryopreserved from blood samples obtained from COVID-19
164 patients suffering from mild ('Mild (outpatient)') or moderate/severe ('Moderate (inpatient)')
165 disease or were already recovered ('Convalescent') and from healthy controls ('HC').
166 Classification of disease severity for this analysis was based on the requirement of
167 hospitalization. Patients with mild COVID-19 were recruited within three days after
168 confirmation of infection by RT-qPCR. From moderate to severe COVID-19 patient blood
169 samples were collected one week after their admittance. The moderate patients were admitted
170 to the hospital requiring medical care, however, they did not need ventilation or O_2 supply.
171 Recovered patients were included based on a positive SARS-CoV-2 antibody testing. Study
172 participant characteristics are described in Table 2.
173
174 *Immunophenotyping of COVID-19 mild, moderate and convalescent COVID-19 patients*
175
176 To compare the number of lymphocytes and monocytes amongst the four study groups,
177 PBMCs were stained and analysed by flow cytometry. Both, lymphocytes (p=0.005) and
178 monocytes (p=0.04), were significantly decreased in moderate COVID-19 patients compared
179 with HC (Suppl. Fig. 1a, b). However, mild and convalescent patients also had a reduced, but
180 not significantly reduced, count of lymphocytes/monocytes compared to HC.
181
182 *Increased inflammatory monocytes and reduced NK cells in moderate COVID-19 patients*
183
184 Monocytes were further classified into classical, non-classical and intermediate based on
185 expression of CD14 and/or CD16 and we used the same gating strategies as described
186 earlier[44] (Suppl. Fig. 1c). We found that $CD16^{++}CD14^{+}$ patrolling (non-classical) monocytes
187 were significantly increased (p=0.0008) in numbers in moderate patients compared to HC,
188 whereas this number is decreased again significantly compared with convalescent patients
189 (p=0.01) (Fig. 1a). The percentage of $CD16^{++}CD14^{+}$ monocytes was also significantly
190 increased (p=0.006) in mild patients (outpatients) compared with moderate patients (Fig. 1a
191 Panel I). Interestingly, $CD16^{++}CD14^{++}$ pro-inflammatory monocytes (intermediate) were again

192 significantly increased in moderate (p=0.003) compared with HC as well as between mild and
193 HC (p=0.02) (Fig. 1a panel II). Furthermore, we observed a significantly reduced percentage
194 of $CD14^{++}CD16^{-}$ phagocytic monocytes (classical) in moderate compared with mild
195 (p=0.0009), HC (p<0.0001) and convalescent (p=0.0003) patients (Fig. 1a Panel III). Finally,
196 we explored the lymphoid cells compartment for NK cells ($CD56^{+}CD3^{-}CD19^{-}$). We found that
197 both mild (p=0.0003) and moderate (p=0.0002) patients were significantly different from
198 convalescent and HC (p<0.0001; HC *vs* mild or moderate) patients (Fig. 1b).
199
200 *Dynamics of B and T cells in mild, moderate and convalescent patients*
201
202 Both T and B cells are indispensable for the immune response against viral infections such as
203 SARS-CoV-2. Firstly, we compared the number of B cells amongst the study groups, which
204 give rise to virus-specific antibodies (see gating strategy in Suppl. Fig. 1c). The $CD19^{+}CD3^{-}$
205 cells (B cells) were significantly increased in mild (p=0.008; 1.7x times) and moderate
206 (p=0.0008; 1.9x times) patients compared with HC (Fig. 2a). Whilst, B cells were significantly
207 decreased in moderate compared to convalescent (p=0.03) patients (Fig. 2a). Comparing
208 $CD3^{+}CD19^{-}$ lymphocytes among the different patient groups we observed no significant
209 difference. However, there was an increased trend of $CD3^{+}$ cells in the outpatients, inpatients
210 and convalescent groups compared with HC.
211
212 $CD3^{+}$ cells were analysed for the $CD4^{+}$ and $CD8^{+}$ T cell compartment. There was a tendency
213 of increased $CD4^{+}$ T cells for outpatients, inpatients and convalescent patients compared to
214 HC, but no significant difference was observed among any of the groups. $CD8^{+}$ T cells were
215 significantly different between HC compared to moderate (p=0.04) or convalescent (p=0.04)
216 patients (Fig. 2b). Finally, we characterized $CD4^{+}Foxp3^{+}CD45R^{-}$ regulatory T cells (Tregs),
217 however, no significant difference was observed among the different groups (Suppl. Fig. 2).
218
219 *Impaired activation and defective cytotoxic functions of $CD8^{+}$ T cells*
220
221 We found that the percentage of $CD8^{+}$ T cells was decreased in mild and convalescent
222 patients compared to HC. Thus, we explored the activation status of $CD8^{+}$ T cells based on
223 HLA-DR expression. We found that $CD8^{+}$ T cell activation status in all three groups of infected
224 patients were significantly different from HC (mild p=0.01, moderate p=0.009, and
225 convalescent p=0.008, Fig. 3a). We characterized the cytotoxic potential of $CD8^{+}$ T cells based
226 on granzyme B and perforin levels and found that there was a tendency of decreased
227 granzyme B expression in mild, moderate and convalescent patients compared with HC (Fig.
228 3b), however it did not reach significance. Perforin was significantly decreased in convalescent
229 (p=0.03) patients compared with HC (Fig. 3b), although mild patients also had borderline
230 significantly reduced levels (p=0.06). Furthermore, we studied the expression of CD38, a
231 marker of cell activation, which was significantly upregulated in convalescent patients
232 compared with HC (p=0.01), mild (p=0.03) and moderate (p=0.02) patients (Fig. 4a). Similarly,
233 convalescent patients had significantly increased numbers of $CD38^{+}PD\text{-}1^{+}$ cytotoxic $CD8^{+}$ T
234 cells compared with HC (p=0.005), moderate (p=0.002) and mild (p=0.002), which reflects the
235 exhaustion and non-responsiveness (anergy) of $CD8^{+}$ T cells (Fig. 4b). Overall, our data
236 suggested that $CD8^{+}$ T cells have reduced activation, diminished expression of cytotoxic
237 molecules such as perforin and granzyme B and severely exhausted phenotype.
238
239 *Dynamics of metabolites production in mild, moderate and convalescent patient*

PBMCs from all patient groups were subjected to $_1$H-NMR spectroscopy analysis. We identified and quantified a total of 18 metabolites (Fig. 5a). Hereby, unsupervised PCA showed that spectral data from mild and moderate patients formed overlapping clusters clearly distinct from a cluster formed by HC and convalescent patients (Fig. 5b), indicating a strong difference in metabolite levels between infectious state compared to healthy or recovered state. Statistical analysis of the four different groups, revealed that 15 metabolites showed p-values < 0.05, with highest significance for metabolites from the energy metabolism (Fig. 5c, Suppl. Fig. 3 & Table 1). The data indicate a strong consumption of glucose, acetate, formate during infection, while with lactate levels are increased. Furthermore, we also found very high levels of fructose in PBMCs from mild patients, medium concentrations in moderate and, low levels in HC and convalescent patients (Fig. 5c). Furthermore, glutamate was almost abolished in mild and moderate patients, potentially as a consequence of enhanced production of α-ketoglutarate in the TCA cycle in PBMCs *via* glutamate dehydrogenase (Fig. 5c).

To find an association between different metabolites, we applied the variable importance of projection (VIP) score. We found that formate and glucose had the highest score compared to another other metabolites (Fig. 6A). In order to determine if additional metabolites are positively associated with changes in glucose, lactate and fructose, we performed a pattern hunter analysis for all metabolites. We found that high glucose levels correlated with high formate, acetate and glutamate and low lactate and fructose (Fig. 6b), indicating enhanced glycolysis and TCA cycle in PBMCs. Similarly, fructose, that is entered *via* fructose-1-phosphate and dihydroxy acetone phosphate (DAP) into the glycolysis, is correlated positively with lactate and citrate and a decrease in acetate and formate, respectively (Fig. 6b). Interestingly, levels of the ROS scavenger taurine are only positively correlated with lactate and fructose, but not glucose (Fig. 6).

Table 1: Summary of metabolites dysregulated in PBMCs

No	Metabolites	HC	Mild	Moderate	Convalescent
1	Glucose	↑↑	↓↓	↓↓	↑↑
2	Formate	↑↑	↓↓↓	↓↓	↑↑
3	Acetate	↑	↓↓	↓	↑
4	Lactate	↓↓	↑↑	↑↑	↓↓
5	Fructose	↓	↑↑	↑	↓
6	Glutamate	↑	↓	↓	↑
7	Citrate	↓	↑↑	↑	↓
8	Taurine	↓↓	-	↑↑	↓
9	Creatine	↓	↑	-	-
10	Alanine	↓	-	↑↑	↓
11	Glycine	↑	↓	↓	-
12	Isoleucine	-	↓↓	↓	↑

To find an association between different metabolites, we applied the variable importance of projection (VIP) score. We found that formate and glucose had the highest score compared to other metabolites (Fig. 6A). In order to determine if additional metabolites are positively associated with changes in glucose, lactate and fructose, we performed a pattern hunter analysis for all metabolites. We found that high glucose levels correlated with high formate,

acetate and glutamate and low lactate and fructose (Fig. 6b), indicating enhanced glycolysis and TCA cycle in PBMCs. Similarly, fructose, that is entered *via* fructose-1-phosphate and dihydroxy acetone phosphate (DAP) into the glycolysis, is correlated positively with lactate and citrate and a decrease in acetate and formate, respectively (Fig. 6b). Interestingly, levels of the ROS scavenger taurine are only positively correlated with lactate and fructose, but not glucose (Fig. 6).

Discussion:

SARS-CoV-2 infections are an intense and rapidly evolving area of research due to the ongoing global pandemic[19,25]. In this study, we used flow cytometry and $_1$H-NMR to decipher the cell proportions and functional state of immune cells (PBMCs) in mild, moderate and convalescent COVID-19 patients compared to HC. Recent reports from COVID-19 patients suggested that mild and severe patient had lymphopenia[11,45-47]. Here, we found that mild patients have reduced lymphocyte numbers whereas convalescent patients have recovered the total lymphocyte counts. Similarly, monocytes were also reduced in mild patients, which is in agreement with other recent studies[29,48,49]. Importantly, our characterization of myeloid cell compartment based on CD16 and CD14 markers suggested that non-classical and intermediate monocytes were increased during an active mild or moderate SARS-CoV-2 infection, once infections are cleared the monocyte numbers return to normal. These results are in accordance with some of the recent published studies[48,50,51], while another study suggested the opposite[52].

In our cohort, specifically CD56$^+$NK cells were dramatically decreased during the course of active SARS-CoV-2 viral infections (mild and moderate), while during recovery the numbers were comparable to HC as report by others[53]. Similarly another recent study suggested the decrease in number of NK cell subsets in COVID-19 patients, with no change in CD56$_{bright}$ or CD56$_{dim}$ cells[54]. Thus, these data point to a crucial role of CD56$^+$NK cells in eliminating SARS-CoV-2 infections[47]. CD19$^+$ B lymphocytes were increased during the course of infection and remain slightly higher than HC, thus reflecting the antibody response against the COVID-19 virus. Thus, this data implicated that these patients were able to generate the SARS-CoV-2 specific B cells.

A major difference was found in the T lymphocytes compartment. On the one hand, CD4$^+$ T cells were increased during infection, but not dramatically. On the other hand, CD8$^+$ T cells were significantly decreased in moderate and convalescent patients as reported earlier[53]. Thus, it appears that during viral infection non-virus specific CD8$^+$ T cells are dead, while the viral-specific surviving CD8$^+$ T cells are clonally expanded but appeared to lost their effector functions[55]. To confirm this, we first measured the activation status of CD8$^+$ T cells and found that CD8$^+$ T appeared to be less activated based on their HLA-DR activation marker[26]. Further, CD8$^+$ T cells were examined for another activation marker CD38 which is involved in cell adhesion, signal transduction and calcium signalling[56] and was found to be upregulated in convalescent patients but not during active infection. These CD38$^+$CD8$^+$ T cells, were also expressing higher levels of PD-1, which is an immune checkpoint and marker of exhaustion[24,30,49,57,58]. It guards against autoimmunity, promotes apoptosis of antigen-specific T cells and promotes self-tolerance by suppressing T cell inflammatory activity. Thus, viral infection leaves convalescent patients with exhausted phenotypes. We found that although there was not a significant change in the numbers of Tregs in COVID-19 patients, there was

322 a trend towards elevated levels of Tregs in COVID-19 patients and rescued Tregs in
323 convalescent patients, in agreement with previous studies[57].
324
325 A key finding of our study was the surprising observation that granzyme B and perforin
326 secreting $CD8_+$ T cells were significantly reduced in convalescent patients. The possible
327 implication of our finding is that convalescent patients, specifically including cancer patients
328 under treatment, could be susceptible to future opportunistic infections with other viruses
329 including different strains of SARS-CoV-2.
330
331 To date, the general metabolic physiology of PBMCs is not well defined in literature. However,
332 it is clear that PBMCs are dependent on circulating nutrients and hormones in the blood
333 system[59]. The defective immune response in COVID-19 patients prompted us to investigate
334 the metabolic functions of these immune cells. Our metabolomics data indeed shows that
335 PBMCs from actively infected patients have a distinct metabolic profile from convalescent or
336 healthy individuals. The most notable difference we observed were for metabolites from the
337 glycolysis and oxidative phosphorylation (TCA cycle) pathway, which is in accordance with
338 recently published transcriptome data for PBMCs[39,43]. Metabolites such as glucose, formate,
339 acetate and choline were also reduced in PBMCs in infected patients whereas, HC and
340 convalescent patients had a normal profile. Accordingly, the glycolytic pathway end products
341 such as lactate were higher in active mild and moderate COVID-19 patients compared with
342 HC and convalescent individuals. Therefore, our data suggests that PBMCs (which constitute
343 a major fraction of T lymphoid cells: 70- 80%) may have changed their metabolic functions,
344 particularly favouring the oxidative phosphorylation pathway over the glycolytic pathway, to
345 meet the high demands of energy needed to combat the ongoing viral infection.
346
347 A recent report suggested that elevated glucose levels enhance SARS-CoV-2 replication and
348 cytokine expression in monocytes and glycolysis sustains the viral-induced monocyte
349 response[60]. Recently, it was emphasized that glucose consumption in PBMCs during COVID-
350 19 disease could be also a read-out of cytokine storms[34]. Further, a higher abundance of
351 citrate in PBMCs suggested that perhaps T cells could use the oxidative phosphorylation
352 pathway for energy consumption to endure the infection, as recent transcriptomic data also
353 suggested that higher expression of genes related to oxidative phosphorylation both in
354 peripheral mononuclear leukocytes and bronchoalveolar lavage fluid (BALF) could play a
355 crucial role in increased mitochondrial activity during SARS-CoV-2 infection[34].
356
357 Another interesting finding of our study was the increase of fructose levels in PBMCs during
358 the course of infection. Previous findings suggested that fructose is involved in the
359 inflammatory pathways for the production of IL-1β and IL-6 production[61]. Thus, it is possible
360 that the immune cells (most probably monocytes) could be triggered by higher fructose and
361 simultaneously induce inflammation and IFN-γ production by T cells[61]. These findings are
362 correlating with recent transcriptomic studies on the BALF from infected COVID-19 patients
363 and plasma of COVID-19 patients that also identified changes in fructose metabolism[34,62].
364
365 We finally observed a reduction of granzyme B and perforin in $CD8_+$ T cells and detected the
366 antioxidant amino acid taurine, which could be involved in the cytotoxic functions of $CD8_+$ T
367 cells. Both granzyme B and perforin are involved in ROS production and taurine serves as
368 ROS scavenger[63,64]. Thus, decreased granzyme B and perforin could be implicated in reduced
369 ROS production for the impaired effectiveness of $CD8_+$ T cells in convalescent or COVID-19

370 patients. This should be the case, as taurine levels that are generally increased during an
371 active infection in mild patients compared to healthy controls are not specifically decreasing
372 due to granzyme B and perforin lacking ROS activity in COVID-19 patients. However, this
373 finding needs further investigation to validate this hypothesis. In summary, the metabolomics
374 data generated in this study provides first and crucial insights into the complex metabolic
375 changes of PBMCs during SARS-CoV-2 infections, warranting further investigation.
376
377 **Conclusions:**
378 Using immunophenotyping and metabolomics approaches we detected significant changes in
379 PBMC samples of mildly and moderately affected COVID-19 as well as convalescent patients
380 compared to healthy controls. The significantly reduced amount of NK cells in both mild and
381 moderate patient groups corresponded with the clustering of PBMCs metabolite levels in the
382 principal component analysis distinct from the cluster formed by healthy and convalescent
383 individuals. The dramatic changed metabolic activity and pathways, such as glycolysis and
384 TCA cycle, might not only lead to a vulnerability of COVID-19 patients to subsequent
385 infections, but can also offer insights into how PBMCs could be manipulated towards a better
386 survival and personalized treatment of moderate and severe COVID-19 patients.
387
388 **Materials and Methods:**
389
390 **Ethics statement**
391 The study protocols were approved by the University of Tübingen, Germany Human Research
392 Ethics Committee (TÜCOV: 256/2020BO2 (convalescent study), COMIHY: (225/2020AMG1)
393 (outpatient study)-COMIHY, EUDRA-CT: 2020-001512-26, ClinicalTrials.gov
394 ID: NCT04340544, and COV-HCQ: (190//2020AMG1) (inpatient study)-COV-HCQ, EUDRA-
395 CT: 2020-001224-33, ClinicalTrials.gov ID: NCT04342221, 556/2018BO2) and all associated
396 procedures were carried out in accordance with approval guidelines. All participants provided
397 written informed consent in accordance with the Declaration of Helsinki.
398
399 **Study participants**
400
401 SARS-CoV-2 positive patients were used for this study and no other virus species were
402 analysed in this study (COMIHY and COV-HCQ). Blood was collected from COVID-19 patients
403 enrolled into two different prospective randomized, placebo-controlled, double blind clinical
404 trials evaluating safety and efficacy of hydroxychloroquine in COVID-19 outpatients
405 (COMIHIY) and hospitalized patients (COV-HCQ). We analysed subsets of these study cohort
406 and used outpatient (n=3; COMIHY) which came to a specified outpatient ward at in the
407 Institute of Tropical Medicine with mild symptoms and blood was taken and usually defined as
408 D1 outpatients. Inpatients (n=3; COV-HCQ), blood was taken after 7-9 days after study
409 inclusion defined as D7. These patients had moderate symptoms needing hospital care,
410 however not being transferred to the intensive care unit in the hospital. Furthermore,
411 convalescent COVID-19 patients (n=4) were defined as positive for serum antibody reactive
412 to SARS-CoV-2 and blood was taken when they visited the Institute of Tropical Medicine for
413 testing of antibody levels. Amongst this cohort, 3 persons reported mild fever for 10-11 days
414 and 1 individual reported no fever but found positive for SARS-CoV-2 antibodies. Blood from
415 healthy controls (n=5) was obtained from the hospital blood bank.
416
417
418

419 **Table 2: Overview of study participants**
420

No	COVID-19 status	Blood sampling	COVID-19 severity	Sex	Age
1	Outpatient (mild)	Day1	mild	F	21
2	Outpatient (mild)	Day1	mild	M	59
3	Outpatient (mild)	Day1	mild	F	40
4	Inpatient (moderate)	Day7	Moderate	M	57
5	Inpatient (moderate)	Day7	Moderate	M	47
6	Inpatient (moderate)	Day7	Moderate	F	78
7	Convalescent (Sero +ve)	Convalescent	Recovered, healthy	F	50
8	Convalescent (Sero +ve)	Convalescent	Recovered, healthy	F	24
9	Convalescent (Sero +ve)	Convalescent	Recovered, healthy	M	50
10	Convalescent (Sero +ve)	Convalescent	Recovered, healthy	F	51
11	HC1	-	None	F	36
12	HC2	-	None	M	60
13	HC3	-	None	M	40
14	HC4	-	None	M	37
15	HC5	-	None	M	47

421
422 **Flow cytometry**
423
424 PBMCs were isolated by standard Ficoll method[65]. A total of 1-2 x10^6 PBMCs per participants
425 were used for three FACS panels (Table 2). In brief, cells were stained with surface markers
426 in DPBS (Sigma) with Super Bright stain Buffer (ThermoFisher) for 30 minutes at room
427 temperature (RT). To distinguish between live from dead, the cells were also incubated with
428 LIVE/DEAD Fixable Infra-Red Dead stain (ThermoFisher). After surface staining cells were
429 also stained for intracellular (IC) markers. Before IC staining, cells were fixed for 30-45 minutes
430 and permeabilized for 5 minutes followed by IC antibody incubation for additional 30 minutes
431 at RT. Cells were washed and resuspended in DPBS containing 2%FBS. Fixing of cells was
432 performed irrespective of whether panel was used for IC staining or not to prevent the possible
433 contamination during acquisition of the samples. For each sample 200,000 cells were acquired
434 using BD LSRFortessa (core facility) equipped with 4 lasers (violet, blue and yellow-green and
435 Red). Data were analysed using Flow Jo (Tree Star) and fluorescence minus one controls
436 (FMO) were used for setting up the arbitrary gates for the major cell markers.
437
438
439
440

441 **Table 2: Antibodies and other reagents used for Flow cytometry**
442

No.	Product Name	Clone	Fluorochrome	Product ID	Company
		NK cells and Monocytes (Panel 1)			
1	CD3	UCHT1	eFluor 450	48-0038-42	Thermofisher
2	CD4	SK3	SuperBright 600	63-0047-42	Thermofisher
3	CD8a	SK1	PerCP-eFluor 710	46-0087-42	Thermofisher
4	CD19	HIB19	eFluor 506	69-0199-42	Thermofisher
5	CD45-RA	HI100	PE-Cy7	25-0458-42	Thermofisher
6	HLA-DR	L243	Alexa Fluor647	A51010	Thermofisher
7	CD38	HIT2	PE-eFluor610	61-0389-42	Thermofisher
8	CD56	MEM188	PE	MA119638	Thermofisher
9	CD16	3G8	Super Bright702	67-0166-42	Thermofisher
10	CD14	61D3	Alexa Fluor700	56-0149-42	Thermofisher
11	Foxp3 (IC)	PCH101	FITC	11-4776-42	Thermofisher
		CD8 exhaustion, T helper follicular cells (Tfh) and antibody secreting cell (ASC) (Panel 2)			
1	CD3	UCHT1	eFluor 450	48-0038-42	Thermofisher
2	CD19	HIB19	eFluor 506	69-0199-42	Thermofisher
3	CD4	SK3	Super Bright 600	63-0047-42	Thermofisher
4	CD8a	SK1	PerCP-eFluor 710	46-0087-42	Thermofisher
5	CD38	HIT2	PE-eFluor 610	61-0389-42	Thermofisher
6	CD27	O323	Alexa Fluor700	56-0279-42	Thermofisher
7	CXCR5 (CD185)	MU5UBEE	FITC	11-9185-42	Thermofisher
8	ICOS (CD278)	C398.4A	PE	12-9949-81	Thermofisher
9	PD-1 (CD279)	eBioJ105 (J105)	PE-Cy7	25-2799-42	Thermofisher
10	HLA-DR	L243	Alexa Fluor647	A51010	Thermofisher
		Cytotoxic potential			
1	CD4	SK3	SuperBright600	63-0047-42	Thermofisher
2	CD8	SK1	PerCP-eFluor710	46-0087-42	Thermofisher
3	CD19	HIB19	eFluor 506	69-0199-42	Thermofisher
4	CD38	HIT2	PE-eFluor 610	61-0389-42	Thermofisher
5	HLA-DR	L243	Alexa Fluor 647	A51010	Thermofisher

6	GZMA (IC)	CB9	Alexa Fluor 488		Thermofisher
7	GZMB (IC)	GB11	PE	MA523639	Thermofisher
8	Perforin (IC)	dG9	PE-Cy7	12-9177-42	Thermofisher
		Other Flow reagents			
1	Ultracompensation bead			01-2222-42	Thermofisher
2	FOXP3/TRN FACTOR STAIN BUFFER SET			00-5523-00	Thermofisher
3	FLOW STAIN BUFFER SOLN			00-4222-57	Thermofisher
4	SB COMPLETE STAINING BUFFER			SB-4401-42	Thermofisher
5	DPBS			D8537	Sigma
6	Pancoll human			P04-601000	Pan Biotech

$_1$H-NMR metabolomics

To obtain PBMCs metabolites, PBMCs were suspended in an optimized solvent extraction mixture of 9:1 (methanol:chloroform) as described elsewhere in detail[66] and extracted with a focused ultrasound system (Covaris E220, Woburn, USA). The extraction solutions were evaporated to dryness for 4 hours in a vacuum concentrator and afterwards pellets resuspended with 45 µL in a 1 mM TSP containing deuterated phosphate buffer. After centrifugation at 20,000 x g for 10 min to remove residual macromolecules, 40 µL of the clear supernatant were transferred to 1.7 mm NMR tubes. Spectra were recorded on an ultrashielded 600 MHz spectrometer (Bruker AVANCE III HD, Karlsruhe, Germany) with a triple resonance 1.7 mm room temperature probe. Spectra used for analysis were acquired with a 2h 55min lasting CPMG pulse program. Metabolite annotation and quantification was done with ChenomX NMR Suite 8.3.

Statistical analysis

Bar diagrams were prepared using GraphPad Prism 6.0. FACS data were analysed using one-way ANOVA for multiple group comparisons (mild, moderate, convalescent and HC) in GraphPad Prism software. No matching or pairing was used. Assumed Gaussian distribution with equal standard deviations (SDs) for experimental design. Mean of each group was compared with the mean of every other group and Tukey's post-hoc tests for multiple comparisons. P value considered significant less than 0.05. Metabolites data were analysed with MetaboAnalyst 4.0 software.

Figure legends:

Fig. 1: Comparison of monocytes and NK cell percentage amongst study groups.

A. The stained PBMCs were gated on the monocyte population and $CD3^{+}CD19^{+}$ cells were excluded. Cell populations are displayed for CD16 and CD14 expression (upper FACS panel). One exemplary dot plot is shown per study group. The bar diagrams (lower panel) show the non-classical ($CD16^{++}CD14^{+}$), intermediate ($CD16^{++}CD14^{++}$) and classical ($CD16^{-}CD14^{++}$) monocytes. *P value <0.05, **P value <0.01 and ***P value <0.001.
B. The stained PBMCs were gated on lymphocyte population and further excluded the $CD3^{+}CD19^{+}$ cells and examined for the CD56 and CD16 expression in HC, mild, moderate and convalescent (upper FACS panel). One exemplary dot plot is shown per study group. The bar diagram shows the $CD56^{+}CD3^{-}CD19^{-}$ NK cells. **P value <0.01 and ****P value <0.0001.

Fig. 2: Increased B cells in mild and moderate patients and reduced $CD8^{+}$ cytotoxic T cells in mild and convalescent patients

A. The stained PBMCs were gated on lymphocyte population and examined for the CD19 and CD3 expression in HC, mild, moderate and convalescent (upper FACS panel). One exemplary dot plot is shown per study group. The bar diagram shows $CD3^{-}CD19^{+}$ B cells. *P value <0.05, **P value <0.01 and ***P value <0.001.
B. The $CD19^{-}CD3^{+}$ lymphocytes were examined for $CD4^{+}$ and $CD8^{+}$ T marker expression. One exemplary dot plot is shown per study group. There was statistically significant difference among HC, mild, moderate and convalescent (upper FACS panel). However, $CD8^{+}$ T cells were significantly reduced in outpatient and convalescent patients. *P value <0.05.

Fig. 3: Decreased activation and cytotoxic functional protein expression of $CD8^{+}$ T cells in convalescent patients

A. $CD8^{+}$ T cells were examined for the expression of activation marker HLA-DR (upper FACS panel). One exemplary dot plot is shown per study group. The bar diagram (lower panel) shows that HLA-DR was significantly lower on $CD8^{+}$ T cells in mild, moderate and convalescent COVID-19^{+} patients compared with HC.
B. $CD8^{+}$ T cells were examined for the expression of their cytotoxic potential using granzyme B and perforin expression using IC staining (upper FACS panel). One exemplary dot plot is shown per study group. There was statistically significant difference among HC, mild, moderate and convalescent (upper FACS panel) for granzyme B. The bar diagram (lower panel) shows that perforin expression was significantly lower on $CD8^{+}$ T cells in convalescent COVID-19^{+} patients compared with HC, though mild and moderate represent lower expression of perforin, but it did not to a significant level. *P value <0.05.

Fig. 4: Increased exhausted $CD8^{+}$ T cells in convalescent patients

521 A. Expression of activation marker CD38 on $CD8_+$ T cells (upper FACS panel). One
522 exemplary dot plot is shown per study group. The bar diagram (lower panel) shows
523 that CD38 expression was significantly higher on $CD8_+$ T cells in convalescent COVID-
524 19_+ patients compared with HC. *P value <0.05.
525
526 B. Expression of activation marker CD38 and PD-1 on $CD8_+$ T cells (upper FACS panel).
527 One exemplary dot plot is shown per study group. The bar diagram (lower panel)
528 shows that $PD\text{-}1_+CD38_+$ expression on was significantly higher on $CD8_+$ T cells in
529 convalescent $COVID\text{-}19_+$ patients compared with HC. *P value <0.05, **P value <0.01.
530
531 **Fig. 5:** $_1$H-NMR spectroscopy of PBMC extracts
532 A. Heatmap of featured metabolites' concentrations plotted with SARS-CoV-2
533 progression group clustering.
534 B. Principle component analysis (PCA) was performed to identify the clustering of two
535 different groups. HC and convalescent COVID-19 patient samples cluster together
536 while SARS-Co-2 infected mild and moderate patients cluster in a separate cluster with
537 PC1: 90.7% and PC2: 2.6%.
538 C. Box plots for differentially abundantly present metabolites in different group including
539 HC, mild, moderate, and convalescent COVID-19 patient. *P value <0.05, **P value
540 <0.01 and ***P value <0.001.
541
542 **Fig. 6:** Pattern hunter plots provide an insight of close correlations with other metabolites
543 during COVID-19 infection.
544 A. Variable Importance in Projection (VIP) scores for all metabolites in the four studied
545 groups.
546 B. Pattern hunter plot for glucose.
547 C. Pattern hunter plot for lactate and fructose.
548
549 **Suppl. Fig. 1:** Total % counts of monocytes and lymphocytes from PBMCs of COVID-19
550 patients.
551 A. Fixed PBMCs samples were acquired on flow cytometry on 2-3 different days for the
552 entire experiments. Total 200,000 cells were acquired by flow cytometry and gating
553 was performed based on FSC and SSC parameters for lymphocytes, monocytes and
554 dead cells as described earlier[67-69].
555 B. The bar graphs represent the % of lymphocytes and monocytes.
556 C. Gating strategy for T lymphocytes (CD3, CD4 and CD8) monocytes (CD14 and
557 CD16)[44], NK cells (CD56) using FMO controls.
558
559 **Suppl. Fig. 2:** Kinetics of regulatory T cells is not affected significantly in mild, moderate and
560 convalescent patients.
561
562 $Foxp3_+$ expression on $CD19_-CD3_+CD4_+CD45RA_-$ T cells to identify the regulatory T cells in
563 HC, outpatient, outpatient and convalescent (upper FACS panel). There was statistically
564 significant difference among HC, mild, moderate and convalescent (upper FACS panel).
565
566 **Suppl. Fig. 3:** Metabolite analysis in COVID-19 patients
567 A. Analysis of Variance (ANOVA) for multi-group comparisons
568 B. Partial Least Squares Discriminant Analysis (PLSDA) scores plot

C. Hierarchical clustering of metabolites (distance measured with Pearson r correlation coefficient)
D. Boxplots for branched chain amino acids valine and leucine

Authors contributions:

YS: Overall study design and project coordination, flow cytometry experiments, data analysis and interpretation and initial metabolic sample preparation, funding generation, and writing the manuscript.
CT: Metabolites sample preparation, Processing of the sample on $_1$H-NMR, data analysis, data interpretation and writing
MO: Metabolites sample preparation, Processing of the sample on $_1$H-NMR
RF, NK: Provided patient materials, Isolation of PBMCs, Performed the experiments for flowcytometry in BSL-2 facility, flow data interpretations.
JH, AK: Coordination of the clinical trials, revision of the manuscript.
RB: Isolation of PBMCs from HC and sample preparation for flow cytometry.
SO, MS, NC, OR: Study design, providing research tools, funding generation, data interpretation and writing and amending the manuscript.

All the authors have seen the manuscript, substantially contributed and agreed to be co-author.

Acknowledgements:

We thank you all the patients who participated in this study and FACS core facility (Klinikum-Berg) for accessing the Flow cytometry for the experiments. We acknowledge support by Deutsche Forschungsgemeinschaft (DFG) and Open Access Publishing Fund of University of Tübingen.

Funding:

RB is supported by Deutsche Forschungsgemeinschaft (DFG Project no. 426724658). EKFS (MS), DFG (OR), Ferring Pharmaceutical (YS and MS). Funders have no role in the study design and data analysis. The German Federal Ministry of Education and Research (BMBF) (BMBF-01KI2052) and the German Federal Ministry of Health (BMG) (BMG-ZMVI1-1520COR801).

Competing interests:

Authors declare no financial competing interests.

Consortia

The members of the Deutsche COVID-19 Omics Initiative (DeCOI) are Angel Angelov, Robert Bals, Alexander Bartholomäus, Anke Becker, Daniela Bezdan, Ezio Bonifacio, Peer Bork, Nicolas Casadei, Thomas Clavel, Maria Colome-Tatche, Andreas Diefenbach, Alexander Dilthey, Nicole Fischer, Konrad Förstner, Julia-Stefanie Frick, Julien Gagneur, Alexander Goesmann, Torsten Hain, Michael Hummel, Stefan Janssen, Jörn Kalinowski, René Kallies, Birte Kehr, Andreas Keller, Sarah Kim-Hellmuth, Christoph Klein, Oliver Kohlbacher, Jan O.

Korbel, Ingo Kurth, Markus Landthaler, Yang Li, Kerstin Ludwig, Oliwia Makarewicz, Manja Marz, Alice McHardy, Christian Mertes, Markus Nöthen, Peter Nürnberg, Uwe Ohler, Stephan Ossowski, Jörg Overmann, Silke Peter, Klaus Pfeffer, Anna R. Poetsch, Alfred Pühler, Nikolaus Rajewsky, Markus Ralser, Olaf Rieß, Stephan Ripke, Ulisses Nunes da Rocha, Philip Rosenstiel, Antoine-Emmanuel Saliba, Leif Erik Sander, Birgit Sawitzki, Philipp Schiffer, Eva-Christina Schulte, Joachim L. Schultze, Alexander Sczyrba, Yogesh Singh, Oliver Stegle, Jens Stoye, Fabian Theis, Janne Vehreschild, Jörg Vogel, Max von Kleist, Andreas Walker, Jörn Walter, Dagmar Wieczorek, and John Ziebuhr.

References:

1 Zhu, N. et al. A Novel Coronavirus from Patients with Pneumonia in China, 2019. N Engl J Med 382, 727-733, doi:10.1056/NEJMoa2001017 (2020).

2 Dashboard, J. C.-L. https://coronavirus.jhu.edu/map.html. (2020).

3 Dashboard, W. L. https://covid19.who.int. (2020).

4 Chang, L., Yan, Y. & Wang, L. Coronavirus Disease 2019: Coronaviruses and Blood Safety. Transfus Med Rev, doi:10.1016/j.tmrv.2020.02.003 (2020).

5 Lehner, N. J. M. P. J. How does SARS-CoV-2 cause COVID-19? Science, 510-511 (2020).

6 Liu, J. et al. Community Transmission of Severe Acute Respiratory Syndrome Coronavirus 2, Shenzhen, China, 2020. Emerg Infect Dis 26, doi:10.3201/eid2606.200239 (2020).

7 Singhal, T. A Review of Coronavirus Disease-2019 (COVID-19). Indian J Pediatr 87, 281-286, doi:10.1007/s12098-020-03263-6 (2020).

8 WHO. <WHO-2019-nCoV-Sci_Brief-Transmission_modes-2020.3-eng.pdf>. WHO Report (2020).

9 Rothe, C. et al. Transmission of 2019-nCoV Infection from an Asymptomatic Contact in Germany. N Engl J Med 382, 970-971, doi:10.1056/NEJMc2001468 (2020).

10 Xu, Z. et al. Pathological findings of COVID-19 associated with acute respiratory distress syndrome. The Lancet Respiratory Medicine 8, 420-422, doi:10.1016/s2213-2600(20)30076-x (2020).

11 Wei Huang, J. B., Michelle McNamara, Suraj Saksena, Marsha Hartman, Tariq Arshad, Scott J. Bornheimerand Maurice O'Gorman. Lymphocyte Subset Counts in COVID-19 Patients: A Meta-Analysis. doi:10.1002/cytoa.24172 (2020).

12 Chen, G. et al. Clinical and immunological features of severe and moderate coronavirus disease 2019. J Clin Invest 130, 2620-2629, doi:10.1172/JCI137244 (2020).

13 Shi, Y. et al. COVID-19 infection: the perspectives on immune responses. Cell Death Differ, doi:10.1038/s41418-020-0530-3 (2020).

14 NcA OANA dOcEA, A. T., DANA ALBULEScU, OANA CRISTEA, & OVIdIU ZLATIAN, M. V., STERGHIOS A. MOScHOS, dIMITRIS TSOUKALAS, MARINA GOUMENOU, NIKOLAOS dRAKOULIS, JOSEF M. dUMANOV, VIcTOR A. TUTELYAN, GENNAdII G. ONIScHENKO, MIcHAEL AScHNER, dEMETRIOS A. SPANdIdOS and dANIELA cALINA. A new threat from an old enemy: Re-emergence of coronavirus (Review). INTERNATIONAL JOURNAL OF MOLEcULAR MEdIcINE 45, 1631-1643 (2020).

15 Ong, E. Z. et al. A Dynamic Immune Response Shapes COVID-19 Progression. Cell Host Microbe 27, 879-882 e872, doi:10.1016/j.chom.2020.03.021 (2020).

16 Picchianti Diamanti, A., Rosado, M. M., Pioli, C., Sesti, G. & Lagana, B. Cytokine Release Syndrome in COVID-19 Patients, A New Scenario for an Old Concern: The Fragile Balance between Infections and Autoimmunity. Int J Mol Sci 21, doi:10.3390/ijms21093330 (2020).

17 Vabret, N. et al. Immunology of COVID-19: Current State of the Science. Immunity 52, 910-941, doi:10.1016/j.immuni.2020.05.002 (2020).

18 Velavan, T. P. & Meyer, C. G. Mild versus severe COVID-19: Laboratory markers. Int J Infect Dis 95, 304-307, doi:10.1016/j.ijid.2020.04.061 (2020).

19 Daniela Weiskopf1, K. S. S., Matthijs P. Raadsen, Alba Grifoni, Nisreen M.A. Okba, Henrik Endeman, Johannes P.C. van den Akker, Richard Molenkamp, Marion P.G. Koopmans, Eric C.M. van Gorp, Bart L. Haagmans, Rik L. de Swart, Alessandro Sette, Rory D. de Vries. Phenotype and kinetics of SARS-CoV-2-specific T cells in COVID-19 patients with acute respiratory distress syndrome. Science Immunology, doi:10.1126/sciimmunol.abd2071 (2020). (2020).

20 Del Valle, D. M. et al. An inflammatory cytokine signature predicts COVID-19 severity and survival. Nature Medicine, doi:10.1038/s41591-020-1051-9 (2020).

21 Wu, H. et al. Clinical and Immune Features of Hospitalized Pediatric Patients With Coronavirus Disease 2019 (COVID-19) in Wuhan, China. JAMA Netw Open 3, e2010895, doi:10.1001/jamanetworkopen.2020.10895 (2020).

22 Du, S. Q. & Yuan, W. Mathematical modeling of interaction between innate and adaptive immune responses in COVID-19 and implications for viral pathogenesis. J Med Virol, doi:10.1002/jmv.25866 (2020).

23 Giamarellos-Bourboulis, E. J. et al. Complex Immune Dysregulation in COVID-19 Patients with Severe Respiratory Failure. Cell Host Microbe 27, 992-1000 e1003, doi:10.1016/j.chom.2020.04.009 (2020).

24 Braciale, T. J. & Hahn, Y. S. Immunity to viruses. Immunol Rev 255, 5-12, doi:10.1111/imr.12109 (2013).

25 McKechnie, J. L. & Blish, C. A. The Innate Immune System: Fighting on the Front Lines or Fanning the Flames of COVID-19? Cell Host Microbe 27, 863-869, doi:10.1016/j.chom.2020.05.009 (2020).

26 Thevarajan, I. et al. Breadth of concomitant immune responses prior to patient recovery: a case report of non-severe COVID-19. Nature Medicine, doi:10.1038/s41591-020-0819-2 (2020).

27 Assis, R. R. d. et al. Analysis of SARS-CoV-2 Antibodies in COVID-19 Convalescent Plasma using a Coronavirus Antigen Microarray . bioRxiv preprint doi: https://doi.org/10.1101/2020.04.15.043364., doi:10.1101/2020.04.15.043364 (2020).

28 Cao, Y. et al. Potent Neutralizing Antibodies against SARS-CoV-2 Identified by High-Throughput Single-Cell Sequencing of Convalescent Patients' B Cells. Cell 182, 73-84 e16, doi:10.1016/j.cell.2020.05.025 (2020).

29 Qin, C. et al. Dysregulation of immune response in patients with COVID-19 in Wuhan, China. Clin Infect Dis, doi:10.1093/cid/ciaa248 (2020).

30 Song, J. W. et al. Immunological and inflammatory profiles in mild and severe cases of COVID-19. Nat Commun 11, 3410, doi:10.1038/s41467-020-17240-2 (2020).

31 Channappanavar, R., Fett, C., Zhao, J., Meyerholz, D. K. & Perlman, S. Virus-specific memory CD8 T cells provide substantial protection from lethal severe acute respiratory syndrome coronavirus infection. J Virol 88, 11034-11044, doi:10.1128/JVI.01505-14 (2014).

32 Janice Oh, H. L., Ken-En Gan, S., Bertoletti, A. & Tan, Y. J. Understanding the T cell immune response in SARS coronavirus infection. Emerg Microbes Infect 1, e23, doi:10.1038/emi.2012.26 (2012).

33 Bost, P. et al. Host-Viral Infection Maps Reveal Signatures of Severe COVID-19 Patients. Cell, doi:10.1016/j.cell.2020.05.006 (2020).

34 Gardinassi, L. G., Souza, C. O. S., Sales-Campos, H. & Fonseca, S. G. Immune and Metabolic Signatures of COVID-19 Revealed by Transcriptomics Data Reuse. Frontiers in Immunology 11, doi:10.3389/fimmu.2020.01636 (2020).

35 Ayres, J. S. Immunometabolism of infections. Nat Rev Immunol 20, 79-80, doi:10.1038/s41577-019-0266-9 (2020).

36 Thaker, S. K., Ch'ng, J. & Christofk, H. R. Viral hijacking of cellular metabolism. BMC Biol 17, 59, doi:10.1186/s12915-019-0678-9 (2019).

37 Moreno-Altamirano, M. M. B., Kolstoe, S. E. & Sanchez-Garcia, F. J. Virus Control of Cell Metabolism for Replication and Evasion of Host Immune Responses. Front Cell Infect Microbiol 9, 95, doi:10.3389/fcimb.2019.00095 (2019).
38 Gupta, S. S., Wang, J. & Chen, M. Metabolic Reprogramming in CD8+ T Cells During Acute Viral Infections. Frontiers in Immunology 11, doi:10.3389/fimmu.2020.01013 (2020).
39 Shehata, H. M. et al. Sugar or Fat?-Metabolic Requirements for Immunity to Viral Infections. Front Immunol 8, 1311, doi:10.3389/fimmu.2017.01311 (2017).
40 Pallett, L. J., Schmidt, N. & Schurich, A. T cell metabolism in chronic viral infection. Clin Exp Immunol 197, 143-152, doi:10.1111/cei.13308 (2019).
41 Swamy, M. et al. Glucose and glutamine fuel protein O-GlcNAcylation to control T cell self-renewal and malignancy. Nat Immunol 17, 712-720, doi:10.1038/ni.3439 (2016).
42 Liew, C. C., Ma, J., Tang, H. C., Zheng, R. & Dempsey, A. A. The peripheral blood transcriptome dynamically reflects system wide biology: a potential diagnostic tool. J Lab Clin Med 147, 126-132, doi:10.1016/j.lab.2005.10.005 (2006).
43 Xiong, Y. et al. Transcriptomic characteristics of bronchoalveolar lavage fluid and peripheral blood mononuclear cells in COVID-19 patients. Emerg Microbes Infect 9, 761-770, doi:10.1080/22221751.2020.1747363 (2020).
44 Wong, K. L. et al. The three human monocyte subsets: implications for health and disease. Immunol Res 53, 41-57, doi:10.1007/s12026-012-8297-3 (2012).
45 Liu, J. et al. Longitudinal characteristics of lymphocyte responses and cytokine profiles in the peripheral blood of SARS-CoV-2 infected patients. EBioMedicine 55, 102763, doi:10.1016/j.ebiom.2020.102763 (2020).
46 Wang, F. et al. Characteristics of peripheral lymphocyte subset alteration in COVID-19 pneumonia. J Infect Dis, doi:10.1093/infdis/jiaa150 (2020).
47 Wen, W. et al. Immune cell profiling of COVID-19 patients in the recovery stage by single-cell sequencing. Cell Discov 6, 31, doi:10.1038/s41421-020-0168-9 (2020).
48 Zhang, D. et al. COVID-19 infection induces readily detectable morphological and inflammation-related phenotypic changes in peripheral blood monocytes, the severity of which correlate with patient outcome. medRxiv preprint doi: https://doi.org/10.1101/2020.03.24.20042655. , doi:10.1101/2020.03.24.20042655 (2020).
49 Zhou, R. et al. Acute SARS-CoV-2 Infection Impairs Dendritic Cell and T Cell Responses. Immunity, doi:10.1016/j.immuni.2020.07.026 (2020).
50 Silvin, A. et al. Elevated Calprotectin and Abnormal Myeloid Cell Subsets Discriminate Severe from Mild COVID-19. Cell, doi:10.1016/j.cell.2020.08.002 (2020).
51 Takahashi, T. et al. Sex differences in immune responses that underlie COVID-19 disease outcomes. Nature, doi:10.1038/s41586-020-2700-3 (2020).
52 Schulte-Schrepping, J. et al. Severe COVID-19 Is Marked by a Dysregulated Myeloid Cell Compartment. Cell, doi:10.1016/j.cell.2020.08.001 (2020).
53 Jiang, Y. et al. COVID-19 pneumonia: CD8(+) T and NK cells are decreased in number but compensatory increased in cytotoxic potential. Clin Immunol 218, 108516, doi:10.1016/j.clim.2020.108516 (2020).
54 Christopher Maucourant, I. F., Andrea Ponzetta, Soo Aleman, Martin Cornillet, Laura Hertwig Benedikt Strunz, Antonio Lentini, Björn Reinius, Demi Brownlie, Angelica Cuapio Gomez, Eivind Heggernes Ask, Ryan M. Hull, Alvaro Haroun-Izquierdo, Marie Schaffer, Jonas Klingström, Elin Folkesson, Marcus Buggert, Johan K. Sandberg, Lars I. Eriksson, Olav Rooyackers, Hans-Gustaf Ljunggren, Karl-Johan Malmberg, Jakob Michaëlsson, Nicole Marquardt, Quirin Hammer, Kristoffer Strålin, Niklas K. Björkström; and the Karolinska COVID-19 Study Group. Natural killer cell immunotypes related to COVID-19 disease severity. Science Immunology, doi:10.1126/sciimmunol.abd6832 (2020). (2020).
55 Diao, B. et al. Reduction and Functional Exhaustion of T Cells in Patients With Coronavirus Disease 2019 (COVID-19). Front Immunol 11, 827, doi:10.3389/fimmu.2020.00827 (2020).

56 Katsuyama, E. et al. The CD38/NAD/SIRTUIN1/EZH2 Axis Mitigates Cytotoxic CD8 T Cell Function and Identifies Patients with SLE Prone to Infections. Cell Rep 30, 112-123 e114, doi:10.1016/j.celrep.2019.12.014 (2020).
57 Zheng, H. Y. et al. Elevated exhaustion levels and reduced functional diversity of T cells in peripheral blood may predict severe progression in COVID-19 patients. Cell Mol Immunol, doi:10.1038/s41423-020-0401-3 (2020).
58 De Biasi, S. et al. Marked T cell activation, senescence, exhaustion and skewing towards TH17 in patients with COVID-19 pneumonia. Nat Commun 11, 3434, doi:10.1038/s41467-020-17292-4 (2020).
59 Zeng, Y. et al. Peripheral Blood Mononuclear Cell Metabolism Acutely Adapted to Postprandial Transition and Mainly Reflected Metabolic Adipose Tissue Adaptations to a High-Fat Diet in Minipigs. Nutrients 10, doi:10.3390/nu10111816 (2018).
60 Codo, A. C. et al. Elevated Glucose Levels Favor SARS-CoV-2 Infection and Monocyte Response through a HIF-1alpha/Glycolysis-Dependent Axis. Cell Metab, doi:10.1016/j.cmet.2020.07.007 (2020).
61 Jaiswal, N., Agrawal, S. & Agrawal, A. High fructose-induced metabolic changes enhance inflammation in human dendritic cells. Clin Exp Immunol 197, 237-249, doi:10.1111/cei.13299 (2019).
62 Di Wu, T. S., Xiaobo Yang, Jian-Xin Song Mingliang Zhang Chengye Yao Wen Liu, Muhan Huang, Yuan Yu, Qingyu Yang Tingju Zhu, Jiqian Xu, Jingfang Mu, Yaxin Wang, Hong Wang, Tang Tang, Yujie Ren Yongran Wu, Shu-Hai Lin, Yang Qiu, Ding-Yu Zhang, You Shang, Xi Zhou. Plasma Metabolomic and Lipidomic Alterations Associated with COVID-19. Natl Sci Rev, doi:10.1093/nsr/nwaa086 (2020).
63 Max W. S. Oliveira, J. B. M., Marcos R. de Oliveira, Alfeu Zanotto-Filho, Guilherme A. Behr, Ricardo F. Rocha, José C. F. Moreira, Fábio Klamt. Scavenging and antioxidant potential of physiological taurine concentrations against different reactive oxygen/nitrogen species. Pharmaceutical Reports 62, 185-193 (2010).
64 Cunningham, L., Simmonds, P., Kimber, I., Basketter, D. A. & McFadden, J. P. Perforin and resistance to SARS coronavirus 2. J Allergy Clin Immunol 146, 52-53, doi:10.1016/j.jaci.2020.05.007 (2020).
65 Maskus, D. J. et al. Characterization of a novel inhibitory human monoclonal antibody directed against Plasmodium falciparum Apical Membrane Antigen 1. Sci Rep 6, 39462, doi:10.1038/srep39462 (2016).
66 Lorenz, M. A., Burant, C. F. & Kennedy, R. T. Reducing time and increasing sensitivity in sample preparation for adherent mammalian cell metabolomics. Anal Chem 83, 3406-3414, doi:10.1021/ac103313x (2011).
67 Marimuthu, R. et al. Characterization of Human Monocyte Subsets by Whole Blood Flow Cytometry Analysis. J Vis Exp, doi:10.3791/57941 (2018).
68 Autissier, P., Soulas, C., Burdo, T. H. & Williams, K. C. Evaluation of a 12-color flow cytometry panel to study lymphocyte, monocyte, and dendritic cell subsets in humans. Cytometry A 77, 410-419, doi:10.1002/cyto.a.20859 (2010).
69 Davies, R., Vogelsang, P., Jonsson, R. & Appel, S. An optimized multiplex flow cytometry protocol for the analysis of intracellular signaling in peripheral blood mononuclear cells. J Immunol Methods 436, 58-63, doi:10.1016/j.jim.2016.06.007 (2016).

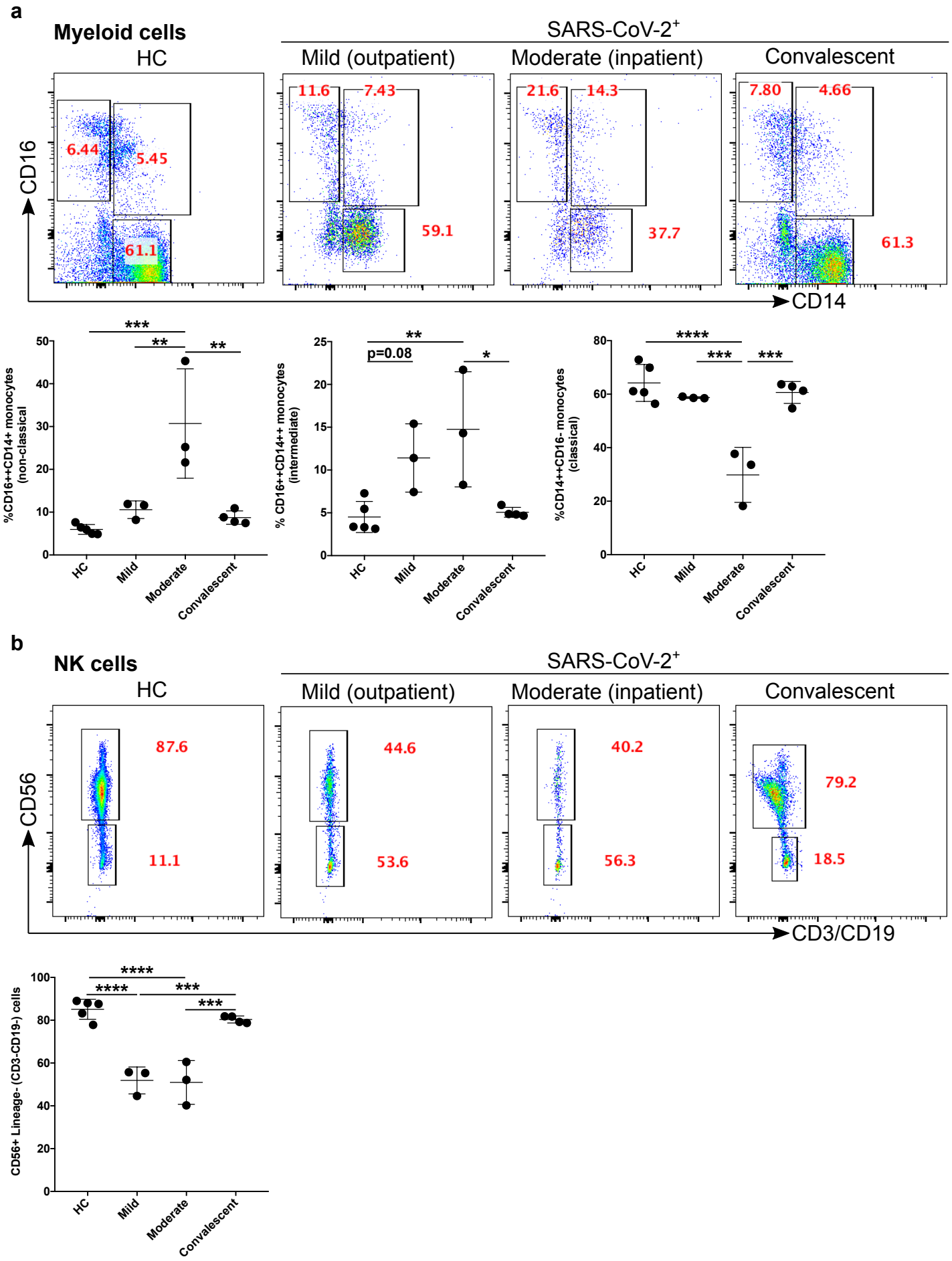
a
Myeloid cells
SARS-CoV-2+
HC
Mild (outpatient)
Moderate (inpatient)
Convalescent
CD16
CD14
6.44
5.45
61.1
11.6
7.43
59.1
21.6
14.3
37.7
7.80
4.66
61.3
%CD16++CD14+ monocytes (non-classical)
% CD16++CD14++ monocytes (intermediate)
%CD14++CD16- monocytes (classical)
p=0.08
HC
Mild
Moderate
Convalescent
b
NK cells
SARS-CoV-2+
HC
Mild (outpatient)
Moderate (inpatient)
Convalescent
CD56
CD3/CD19
87.6
11.1
44.6
53.6
40.2
56.3
79.2
18.5
CD56+ Lineage- (CD3-CD19-) cells
HC
Mild
Moderate
Convalescent

Fig. 1

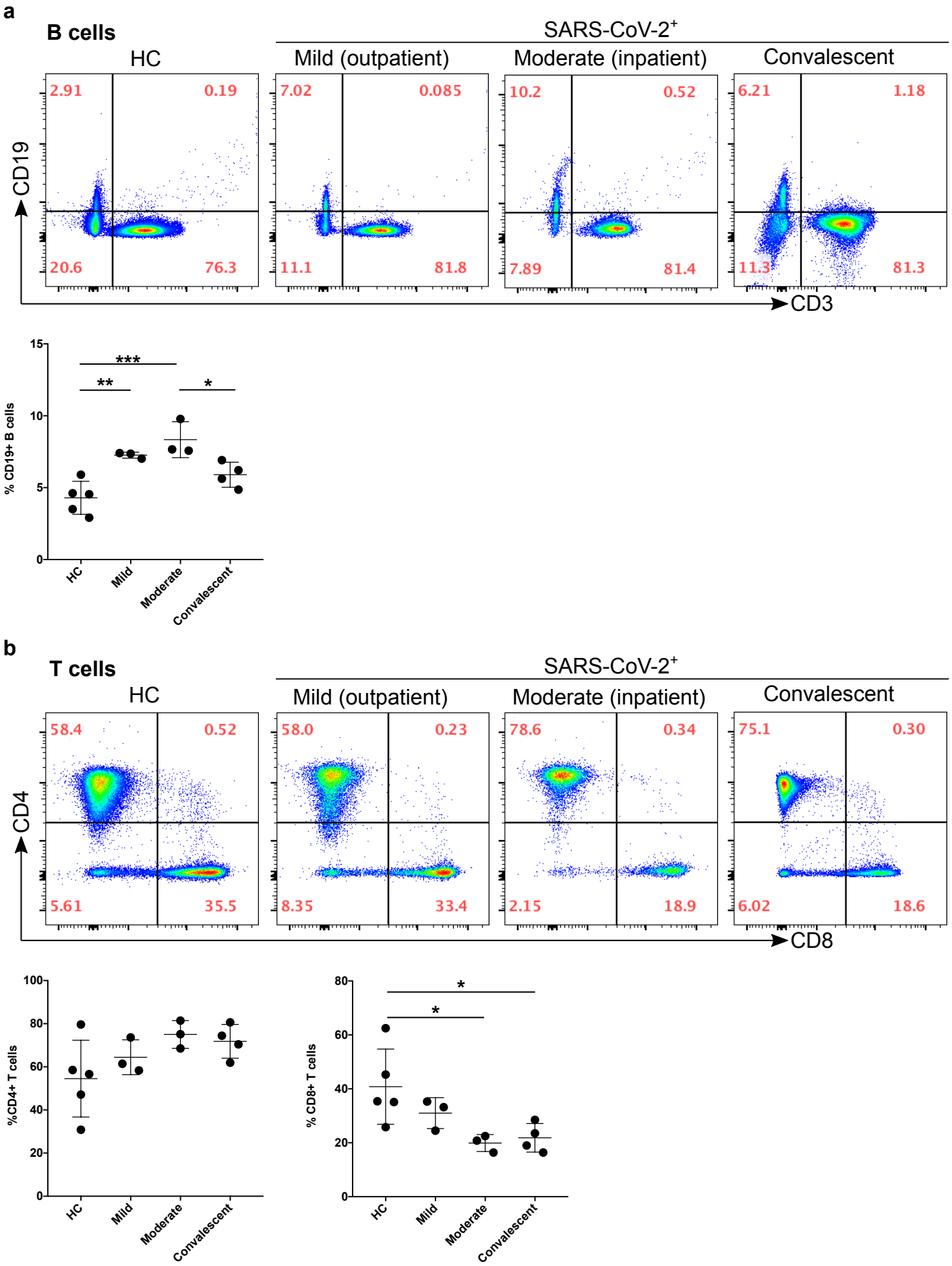
a
B cells
SARS-CoV-2+
HC
Mild (outpatient)
Moderate (inpatient)
Convalescent
2.91
0.19
20.6
76.3
7.02
0.085
11.1
81.8
10.2
0.52
7.89
81.4
6.21
1.18
11.3
81.3
CD19
CD3
% CD19+ B cells
***
**
*
HC
Mild
Moderate
Convalescent
b
T cells
SARS-CoV-2+
HC
Mild (outpatient)
Moderate (inpatient)
Convalescent
58.4
0.52
5.61
35.5
58.0
0.23
8.35
33.4
78.6
0.34
2.15
18.9
75.1
0.30
6.02
18.6
CD4
CD8
%CD4+ T cells
% CD8+ T cells
*
*
HC
Mild
Moderate
Convalescent

Fig. 2

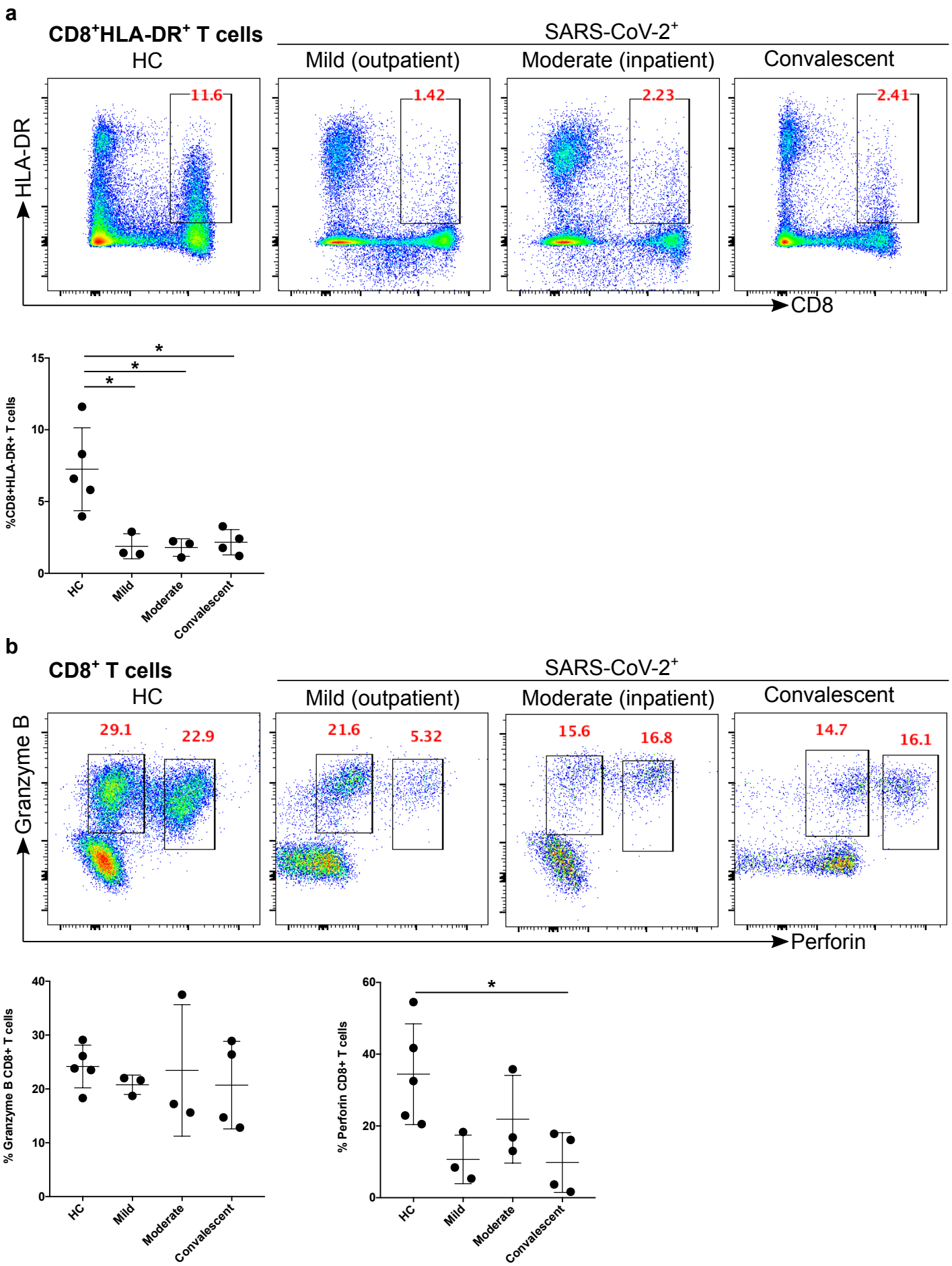
a
CD8+HLA-DR+ T cells
SARS-CoV-2+
HC
Mild (outpatient)
Moderate (inpatient)
Convalescent
11.6
1.42
2.23
2.41
HLA-DR
CD8
%CD8+HLA-DR+ T cells
HC
Mild
Moderate
Convalescent
b
CD8+ T cells
SARS-CoV-2+
HC
Mild (outpatient)
Moderate (inpatient)
Convalescent
29.1
22.9
21.6
5.32
15.6
16.8
14.7
16.1
Granzyme B
Perforin
% Granzyme B CD8+ T cells
% Perforin CD8+ T cells
HC
Mild
Moderate
Convalescent

Fig. 3

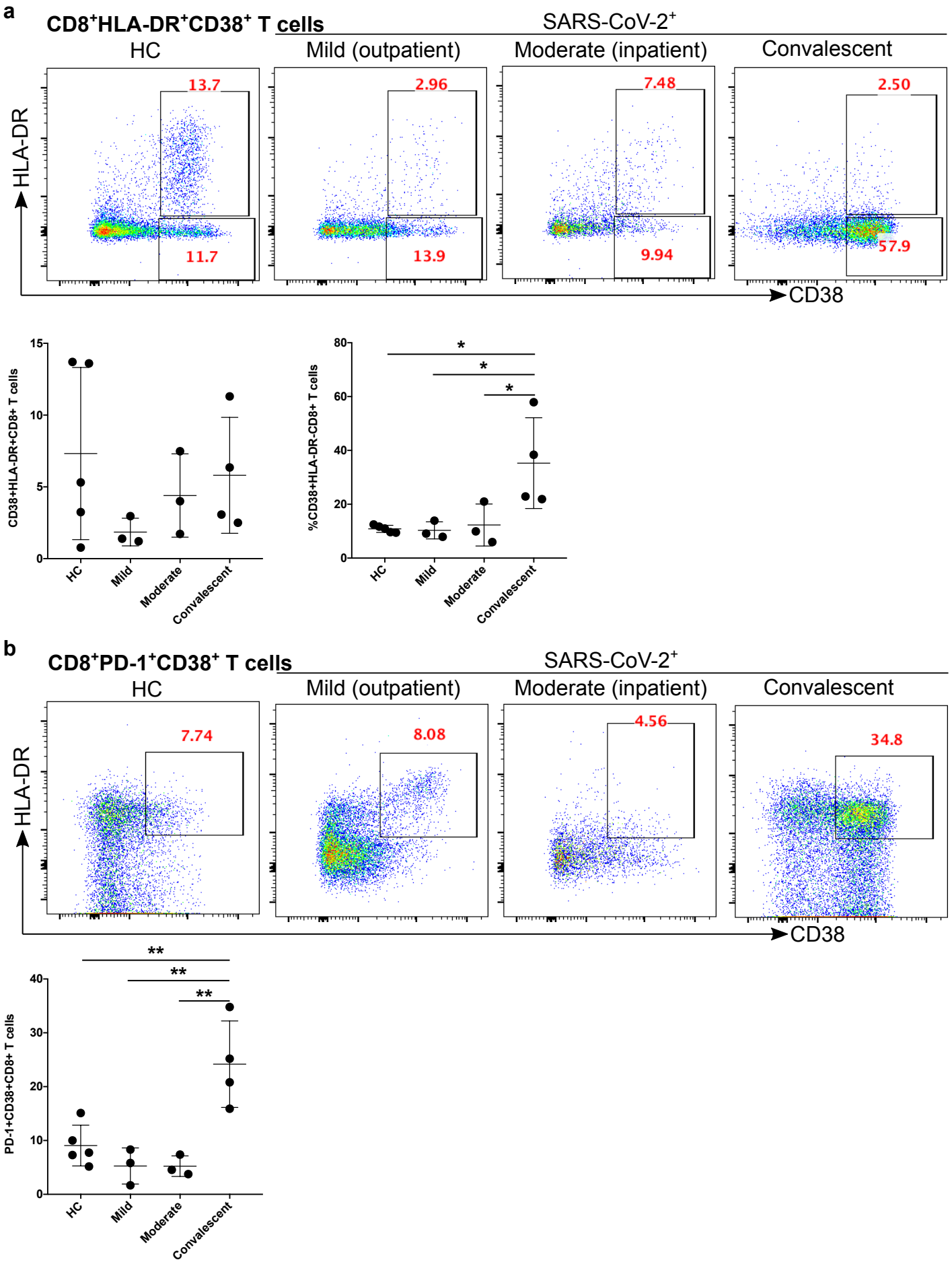
a
CD8+HLA-DR+CD38+ T cells
SARS-CoV-2+
HC
Mild (outpatient)
Moderate (inpatient)
Convalescent
HLA-DR
CD38
13.7
11.7
2.96
13.9
7.48
9.94
2.50
57.9
CD38+HLA-DR+CD8+ T cells
%CD38+HLA-DR-CD8+ T cells
HC
Mild
Moderate
Convalescent
b
CD8+PD-1+CD38+ T cells
SARS-CoV-2+
HC
Mild (outpatient)
Moderate (inpatient)
Convalescent
HLA-DR
CD38
7.74
8.08
4.56
34.8
PD-1+CD38+CD8+ T cells
HC
Mild
Moderate
Convalescent

Fig. 4

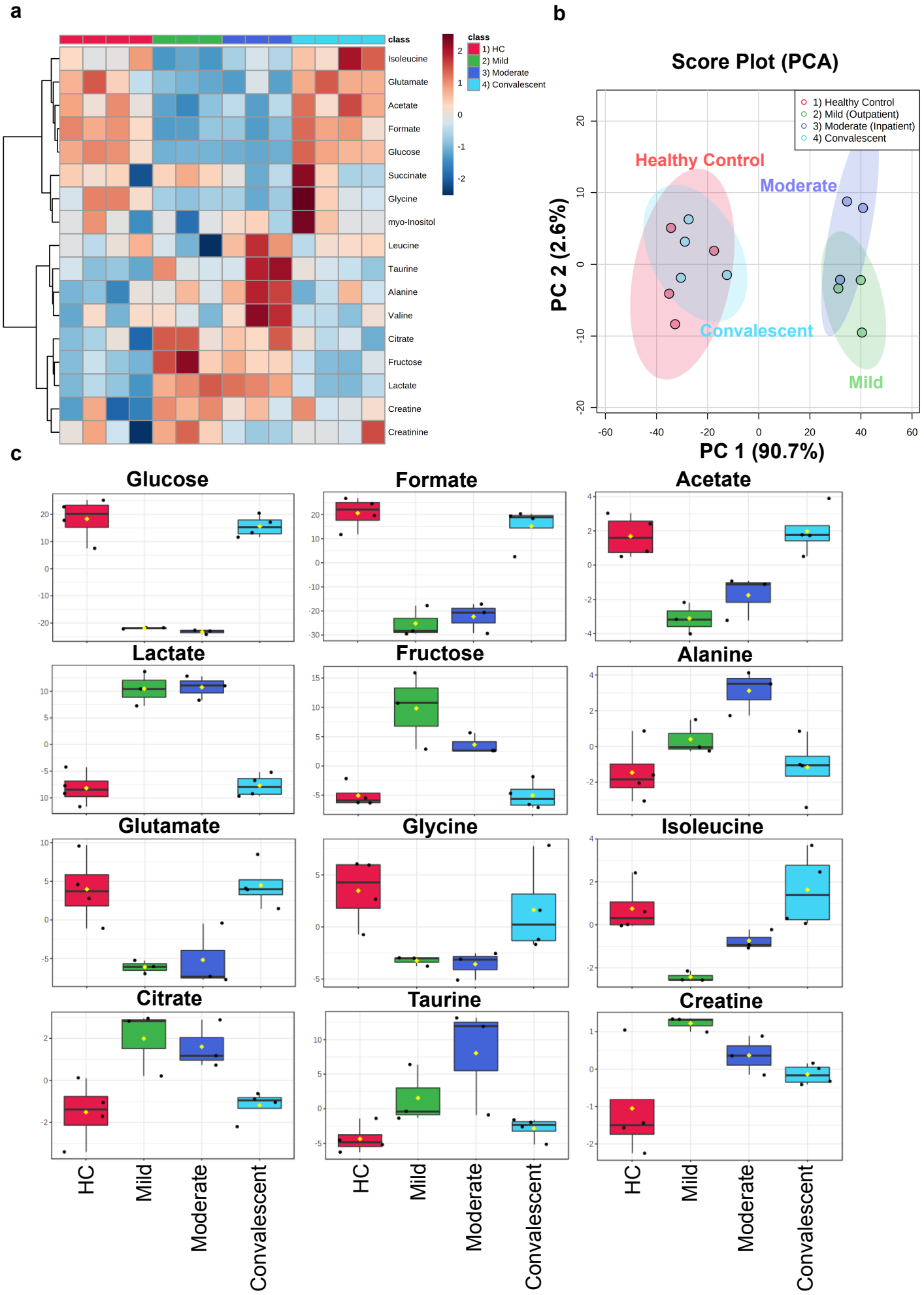
a
class
Isoleucine
Glutamate
Acetate
Formate
Glucose
Succinate
Glycine
myo-Inositol
Leucine
Taurine
Alanine
Valine
Citrate
Fructose
Lactate
Creatine
Creatinine
class
1) HC
2) Mild
3) Moderate
4) Convalescent
b
Score Plot (PCA)
1) Healthy Control
2) Mild (Outpatient)
3) Moderate (Inpatient)
4) Convalescent
Healthy Control
Moderate
Convalescent
Mild
PC 2 (2.6%)
PC 1 (90.7%)
c
Glucose
Formate
Acetate
Lactate
Fructose
Alanine
Glutamate
Glycine
Isoleucine
Citrate
Taurine
Creatine
HC
Mild
Moderate
Convalescent

Fig. 5

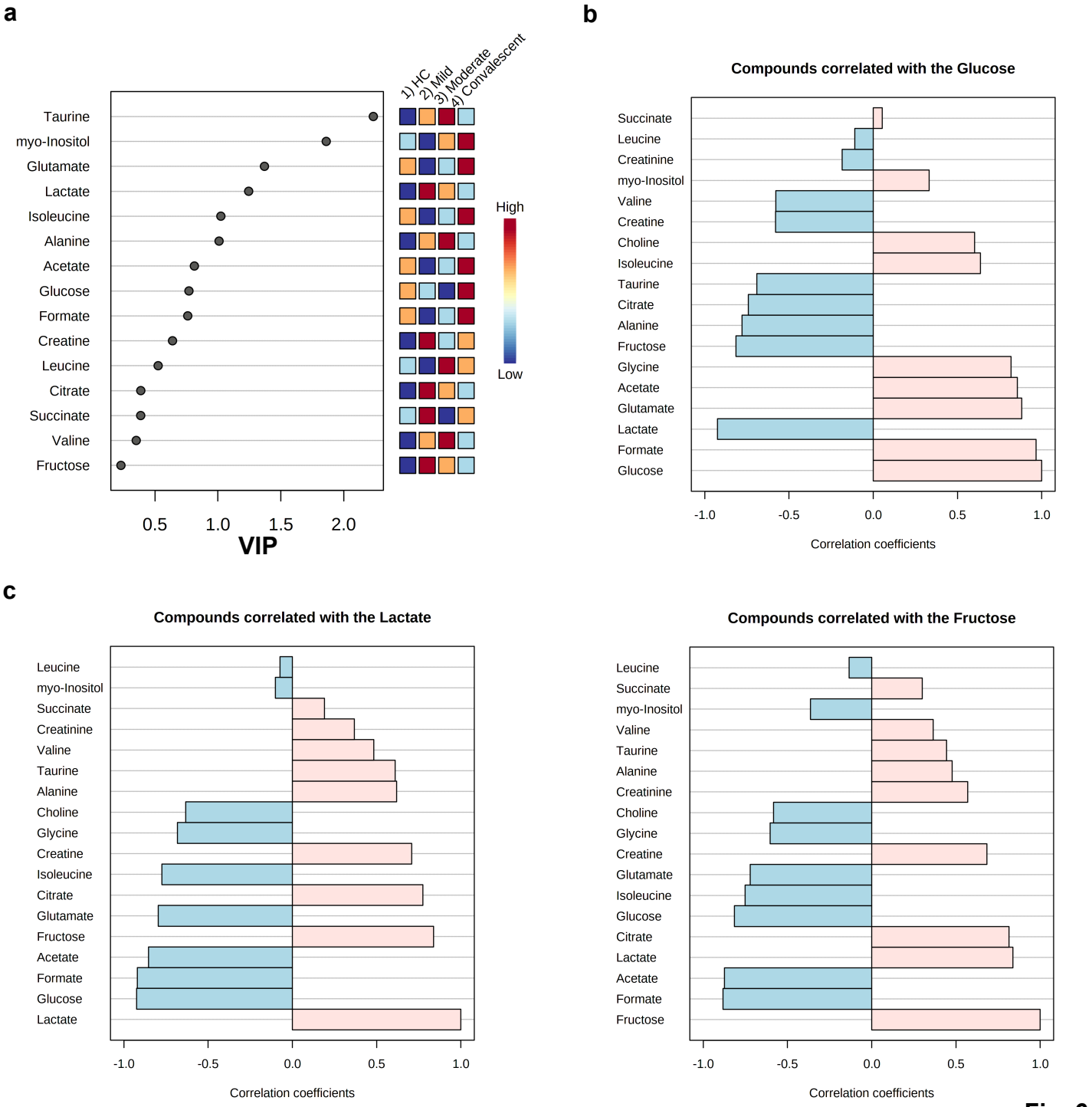
a
Taurine
myo-Inositol
Glutamate
Lactate
Isoleucine
Alanine
Acetate
Glucose
Formate
Creatine
Leucine
Citrate
Succinate
Valine
Fructose
0.5
1.0
1.5
2.0
VIP
1) HC
2) Mild
3) Moderate
4) Convalescent
High
Low
b
Compounds correlated with the Glucose
Succinate
Leucine
Creatinine
myo-Inositol
Valine
Creatine
Choline
Isoleucine
Taurine
Citrate
Alanine
Fructose
Glycine
Acetate
Glutamate
Lactate
Formate
Glucose
-1.0
-0.5
0.0
0.5
1.0
Correlation coefficients
c
Compounds correlated with the Lactate
Leucine
myo-Inositol
Succinate
Creatinine
Valine
Taurine
Alanine
Choline
Glycine
Creatine
Isoleucine
Citrate
Glutamate
Fructose
Acetate
Formate
Glucose
Lactate
-1.0
-0.5
0.0
0.5
1.0
Correlation coefficients
Compounds correlated with the Fructose
Leucine
Succinate
myo-Inositol
Valine
Taurine
Alanine
Creatinine
Choline
Glycine
Creatine
Glutamate
Isoleucine
Glucose
Citrate
Lactate
Acetate
Formate
Fructose
-1.0
-0.5
0.0
0.5
1.0
Correlation coefficients

Fig. 6

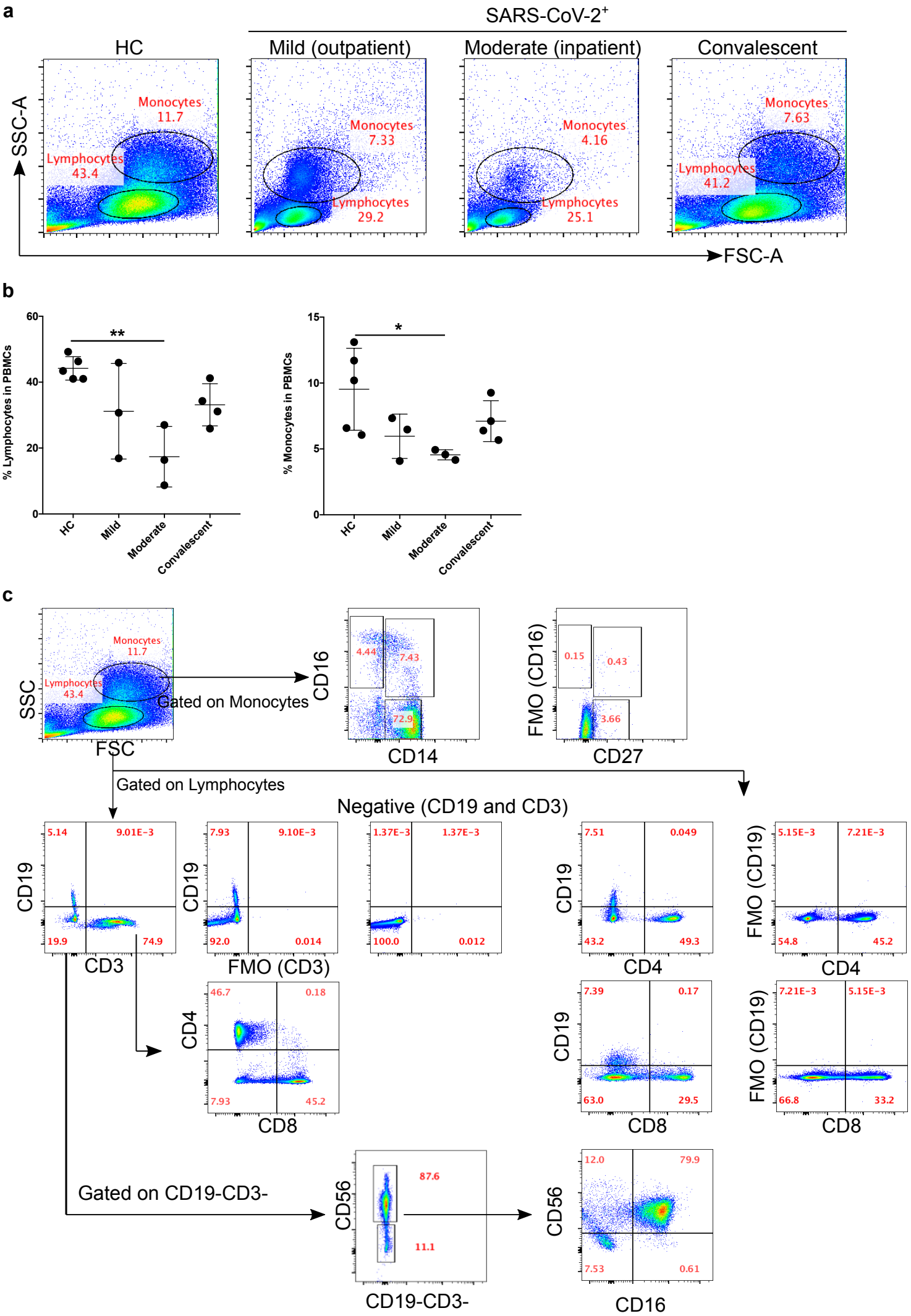
a
SARS-CoV-2+
HC
Mild (outpatient)
Moderate (inpatient)
Convalescent
SSC-A
FSC-A
Monocytes 11.7
Lymphocytes 43.4
Monocytes 7.33
Lymphocytes 29.2
Monocytes 4.16
Lymphocytes 25.1
Monocytes 7.63
Lymphocytes 41.2
b
% Lymphocytes in PBMCs
% Monocytes in PBMCs
HC
Mild
Moderate
Convalescent
c
Gated on Monocytes
CD16
CD14
FMO (CD16)
CD27
Gated on Lymphocytes
Negative (CD19 and CD3)
CD19
CD3
FMO (CD3)
CD4
CD8
FMO (CD19)
Gated on CD19-CD3-
CD56
CD19-CD3-
CD16

Suppl. Fig. 1

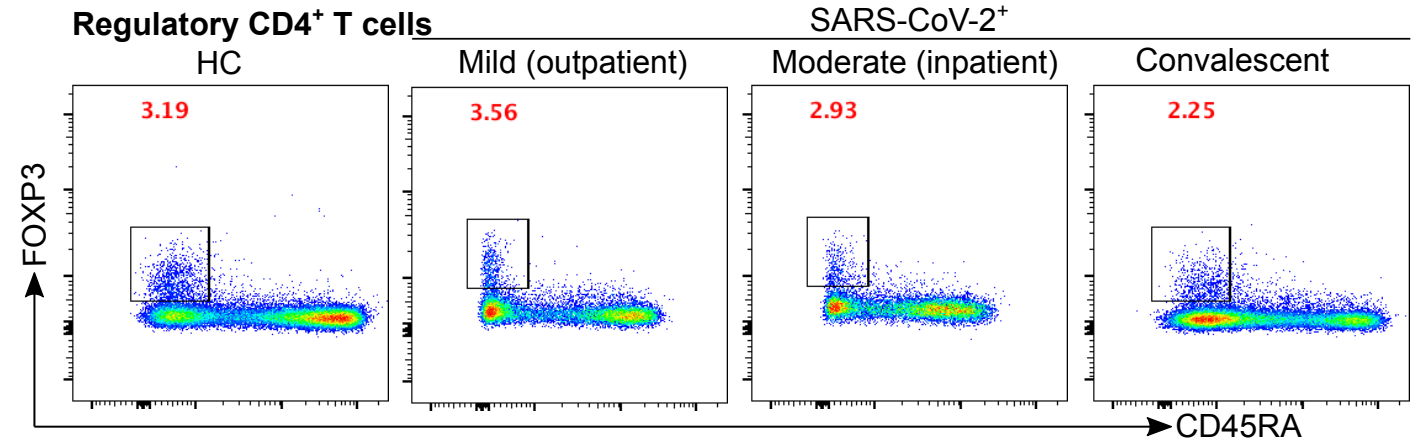
Regulatory CD4+ T cells
SARS-CoV-2+
HC
Mild (outpatient)
Moderate (inpatient)
Convalescent
3.19
3.56
2.93
2.25
FOXP3
CD45RA

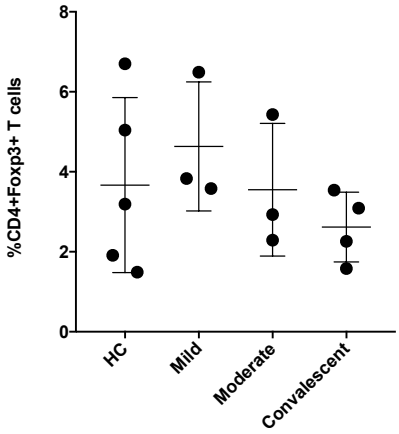
%CD4+Foxp3+ T cells
0
2
4
6
8
HC
Mild
Moderate
Convalescent

Suppl. Fig. 2

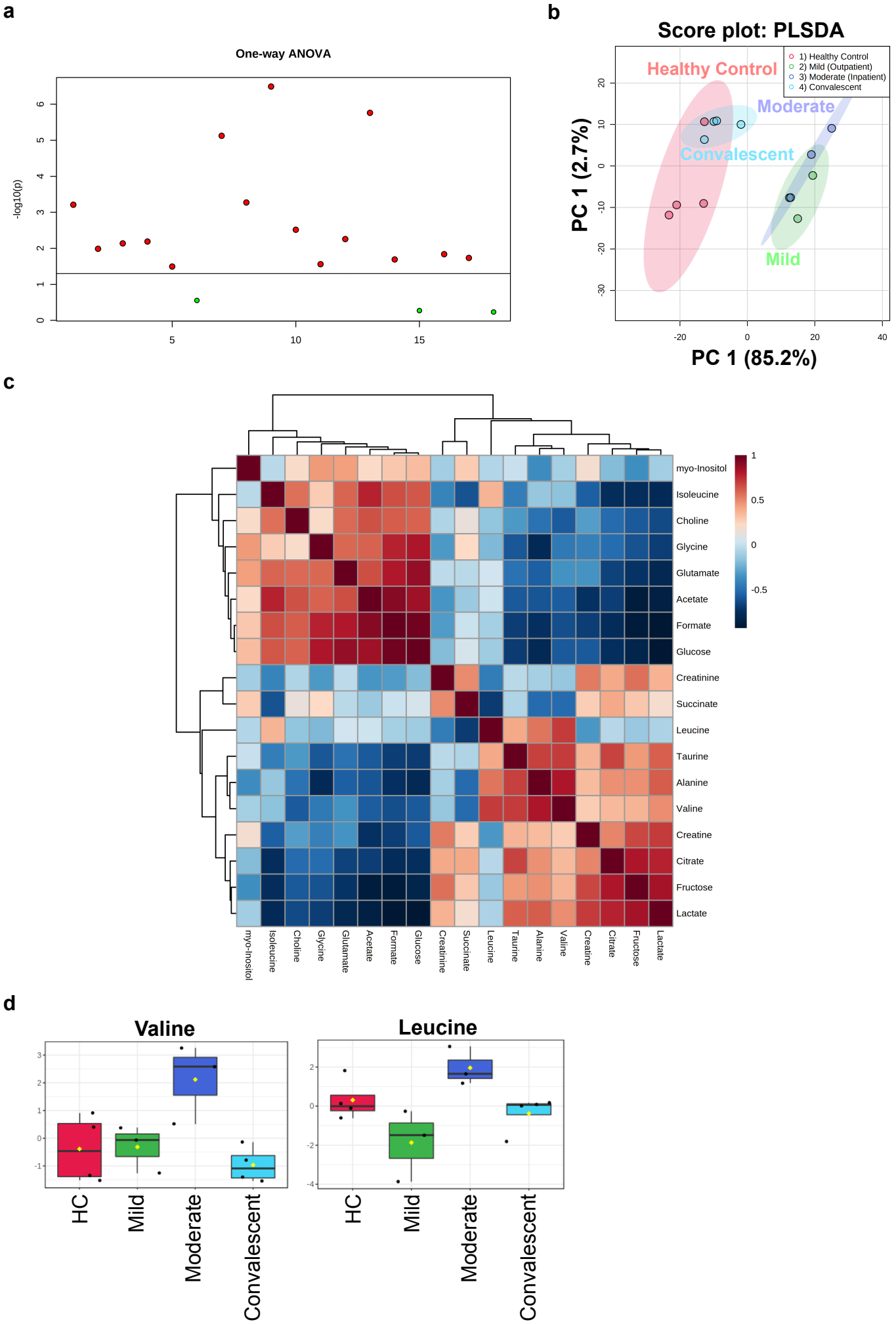
a
One-way ANOVA
-log10(p)
b
Score plot: PLSDA
1) Healthy Control
2) Mild (Outpatient)
3) Moderate (Inpatient)
4) Convalescent
Healthy Control
Moderate
Convalescent
Mild
PC 1 (2.7%)
PC 1 (85.2%)
c
myo-Inositol
Isoleucine
Choline
Glycine
Glutamate
Acetate
Formate
Glucose
Creatinine
Succinate
Leucine
Taurine
Alanine
Valine
Creatine
Citrate
Fructose
Lactate
d
Valine
Leucine
HC
Mild
Moderate
Convalescent

Suppl. Fig. 3